IV. Conclusion

The calculation of eigenmodes in uniform wave guides or in resonant cavities by integral equation and moment method sometimes generates non physical solutions. In this paper a practical criterion for a correct choice of the weighting functions is demonstrated. Its rigorous implementation would be calculus intensive but we show that an approximate implementation efficiently eliminates spurious solutions generated by the conventional Galerkin's method without lengthening computations.

References

[1] S. Sorrentino and T. Itoh, "Transverse resonance analysis for finline discontinuities," *IEEE Trans. Microwave Theory Tech.*, vol. MTT-32, pp. 1633–1638, Dec. 1984.

[2] J. Borneman and F. Arndt, "Calculating the characteristic impedance of finlines by transverse resonnance method," *IEEE Trans. Microwave Theory Tech.*, vol. MTT-34, pp. 85–92, Jan. 1986.

[3] C. A. Olley and T. E. Rozzi, "Systematic characterization of the spectrum of the unilateral finline," *IEEE Trans. Microwave Theory Tech.*, vol. MTT-34, pp. 1147–1156, Nov. 1986.

[4] L. P. Schmidt and T. Itoh, "Spectral domain analysis of dominant and higher order modes in finlines," *IEEE Trans. Microwave Theory Tech.*, vol. MTT-28, pp. 981–985, Sept. 1980.

[5] Johnson and J. H. Wang, *Generalized Moment Methods in Electromagnetics.* New York: Wiley, 1991, pp. 92.

[6] I. Bardi and O. Biro, "An efficient finite-element formulation without spurious modes for anisotropic waveguides," *IEEE Trans. Microwave Theory Tech.*, vol. 39, pp. 1133–1139, July 1991.

[7] H. Aubert, B. Souny, and H. Baudrand, "Origin and avoidance of spurious solutions in the transverse resonance method," *IEEE Trans. Microwave Theory Tech.*, vol. 41, pp. 450–456, Mar. 1993.

[8] W. Schroeder and I. Wolff, "Full wave boundary integral analysis of arbitrary integrated transmission lines: Origin and avoidance of spurious solutions," 20th European Microwave Conf., vol. I, Sept. 1990, pp. 829–834.

[9] R. F. Harrington, *Field Computation by Moment Methods.* New York: MacMillan, 1968.

[10] B. Friedman, *Principles and Techniques of Applied Mathematics.* New York: Wiley, 1956.

[11] R. Dautray and J. L. Lions, *Analyse Mathématique et Calcul Numérique pour les Sciences et les Techniques.* Paris, France: Masson, 1984.

[12] C. Cohen-Tannoudji, B. Diu, and F. Laloë, *Mécanique quantique.* Herman, 1973.

[13] B. Souny, "Fonctions de poids pour méthode de moment," Note Interne LEN7-ENAC 1993.

[14] T. Itoh, "Analysis of microstrip resonators," *IEEE Trans. Microwave Theory Tech.*, vol. MTT-22, pp. 946–952, Nov. 1974.

A New FEM Approach for Open Boundary Laplace's Problem

Dong Xingqi and An Tongyi

***Abstract*—An efficient improved finite element method (FEM) is presented for electromagnetic Laplace's problems with open boundary. The whole infinite domain is divided into a set of infinite elements instead of ordinary finite elements. Since a special FEM discretization and FEM solving procedure are used, it can not only take much less computer memory than that the conventional FEM needs, but also avoid the calculation error introduced by the truncated boundary or absorbing boundary condition used in conventional FEM.**

I. Introduction

Recently, FEM has been more and more widely used for many electromagnetic problems with open boundary. Because in FEM the solution domain is discretized with finite elements, only finite domain problems can be handled directly. So, the solution domain with open boundary must be truncated. A relatively simple technique to implement is to select an external boundary with a zero potential to truncate the solution domain. Another alternative is to use an appropriate absorbing boundary condition or infinite element [1]–[3].

This paper presents a new FEM technique for static electromagnetic problems with open boundary. It utilizes a special discretization form to divide the whole infinite domain into infinite triangular elements. So no truncated boundary or absorbing boundary is needed and the calculation error produced by appropriate boundary condition is avoided. As an example, the capacitance matrix for the two coupled microstrips with open-boundary is calculated and the numerical results are compared with those obtained by other methods.

II. New FEM Procedure

We begin with our discussion of a two-dimensional electrostatic open boundary problem. Assuming that the solution domain is Ω_s and its open boundary is Γ_s. We use a regular polygon Γ_0, which contains the solution domain Ω_s, to divide the whole infinite domain Ω into two parts (see Fig. 1). Defining that the region within Γ_0 is Ω_{in} and the one out of Γ_0 is Ω_{out}. Γ_0 may be placed very close to Γ_s. If Γ_s itself is a regular polygon, then it is selected as Γ_0.

A. Analysis of Ω_{in}

Because the region Ω_{in} is a finite domain, it can be treated by conventional FEM. The electromagnetic field distribution can be obtained from the scalar potential $\Phi(x, y)$ satisfying the Laplace's equation with associated Dirichlet or Neumann boundary condition. The region Ω_{in} is subdivided to triangular finite elements and the stiffness matrix K_{in} can be obtained by assembling each element coefficient matrix. Assuming that the number of nodes on Γ_0 is M_0 and the scalar potentials on Γ_0 form a column vector Φ_0 of order M_0, the number of remaining nodes is M_{in} and the corresponding potentials form a column vector Φ_{in} of order M_{in}. Thus, the functional within the region Ω_{in} can be obtained by

$$F_{in} = \frac{1}{2} \begin{pmatrix} \Phi_{in}^T & \Phi_0^T \end{pmatrix} \begin{pmatrix} K_{in}^{11} & K_{in}^{12} \\ K_{in}^{21} & K_{in}^{22} \end{pmatrix} \begin{pmatrix} \Phi_{in} \\ \Phi_0 \end{pmatrix}. \quad (1)$$

Manuscript received January 27, 1994; revised October 2, 1995.

The authors are with the Institute of Microwave Research, East China Normal University, Shanghai 200062, China.

Publisher Item Identifier S 0018-9480(96)00463-2.

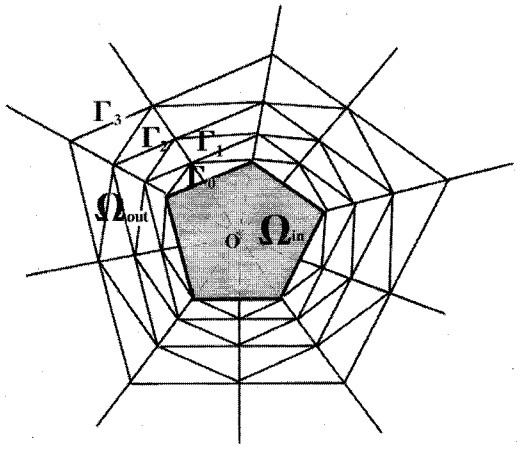

Fig. 1. Similar discretzation of infinite region ω_{out}.

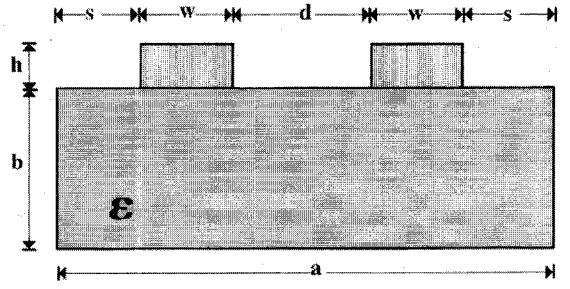

Fig. 2. Coupled microstrips ($\varepsilon = 2\varepsilon_0$, $a = 11b$, $h = b$, $w = 3b$, $d = 2b$, $s = 1.5b$).

B. Analysis of Ω_{out}

The region Ω_{out} is a infinite domain. The FEM discretization is taken as following: first, a coordinate center O within Γ_0 is selected. Next, a set of infinite similar polygons of Γ_0 are taken as shown in Fig. 2. The point O is the similar center of polygons and the constant ξ is similar ratio. The set of similar polygons are denoted as $\Gamma_1, \Gamma_2, \cdots, \Gamma_k, \cdots$ and the region between Γ_{k-1} and Γ_k is denoted as kth layer. Each layer is divided into quadrilaterals of number $M_0 - 1$ by the rays out from similar center point O to nodes on Γ_0. (Note that the polygon apexes must be nodes.) Then each quadrilateral is cut into two triangles. It is necessary that the discretization of every layer is similar as shown in Fig. 1. Assuming that scalar potentials on Γ_k is Φ_k. After the element stiffness matrix is obtained by means of conventional FEM, the layer stiffness matrix can be formed by assembling all finite elements on one layer. It can be written as

$$\begin{pmatrix} K_0 & -A^T \\ -A & K_0' \end{pmatrix} \tag{2}$$

where K_0, K_0', and A are all matrices of order M_0. Because every layer is discretized similarly, all layer stiffnesses are identical. So, if the functional of kth layer is

$$F_k = \frac{1}{2}\begin{pmatrix} \Phi_{k-1}^T & \Phi_k^T \end{pmatrix}\begin{pmatrix} K_0 & -A^T \\ -A & K_0' \end{pmatrix}\begin{pmatrix} \Phi_{k-1} \\ \Phi_k \end{pmatrix} \tag{3}$$

then, the functional of the whole infinite domain Ω_{out} is a infinite sum as

$$F_{out} = \sum_{k=1}^{\infty} F_k. \tag{4}$$

C. Synthesis of Ω_{in} and Ω_{out}

Considering both Ω_{in} and Ω_{out}, the functional of the whole Ω can be written as

$$F = F_{in} + F_{out}. \tag{5}$$

Because the first derivatives of the functional (5) with respect to the node variables should be zero, we can have a set of equations of infinite order

$$\begin{cases} K_{in}^{11}\Phi_{in} + K_{in}^{12}\Phi_0 = 0 \\ K_{in}^{21}\Phi_{in} + K_{in}^{22}\Phi_0 + K_0\Phi_0 - A^T\Phi_1 = 0 \\ -A\Phi_0 + K\Phi_1 - A^T\Phi_2 = 0 \\ \cdots \\ -A\Phi_{k-1} + K\Phi_k - A^T\Phi_{k+1} = 0 \\ \cdots \end{cases} \tag{6}$$

where $K = K_0 + K_0'$. It is impossible to solve the (6) directly. It is easy to prove that there exists a matrix X of order M_0 which satisfies

$$\Phi_{k+1} = X\Phi_k \tag{7}$$

where X is called transfer matrix. Letting $k = 0$, from (6) and (7) we have

$$K_{in}^{21}\Phi_{in} + K_{in}^{22}\Phi_0 + K_0\Phi_0 - A^T X\Phi_0 = 0 \tag{8}$$

$$K_{out} = K_0 - A^T X \tag{9}$$

$$K_{in}^{21}\Phi_{in} + K_{in}^{22}\Phi_0 + K_{out}\Phi_0 = 0. \tag{10}$$

Combining (6) and (10), we have

$$\begin{pmatrix} K_{in}^{11} & K_{in}^{12} \\ K_{in}^{21} & K_{in}^{22} + K_{out} \end{pmatrix}\begin{pmatrix} \Phi_{in} \\ \Phi_0 \end{pmatrix} = 0. \tag{11}$$

Imposing boundary condition within the solution domain Ω_0, the scalar potentials Φ_{in} and Φ_0 can be solved from (11). Then from (7), the scalar potentials Φ_k of the region Ω_{out} can be obtained.

D. Calculation of Transfer Matrix X

Combine (7) with (6), then

$$-A + KX - A^T X^2 = 0. \tag{12}$$

Let

$$R_1 = \begin{pmatrix} K & -A \\ I & 0 \end{pmatrix}$$
$$R_2 = \begin{pmatrix} A^T & 0 \\ 0 & I \end{pmatrix} \tag{13}$$

where I is unit matrix. From (6) we have:

$$R_1\begin{pmatrix} \Phi_k \\ \Phi_{k-1} \end{pmatrix} = R_2\begin{pmatrix} \Phi_{k+1} \\ \Phi_k \end{pmatrix}. \tag{14}$$

Assuming that λ and g are the eigenvalues and eigenvectors of X, then

$$Xg = \lambda g. \tag{15}$$

Letting $k = 1$ and $\Phi_0 = g$ in (14), (14) together with (7) and (15) will take the form

$$R_1\begin{pmatrix} \lambda g \\ g \end{pmatrix} = \lambda R_2\begin{pmatrix} \lambda g \\ g \end{pmatrix}. \tag{16}$$

Equation (16) can now be solved by any standard generalized eigenvalue analysis computer package for the eigenvalues of number

TABLE I
CAPACITANCE MATRIX FOR THE COUPLED MICROSTRIPS OF FIG. 2

	Reference [6]	Shield [4]	ABC [4]	Higher Order ABC[4]	Infinite FEM [5]	the paper
C_{11} 10^{-10}	0.9224	1.091	0.9249	0.9230	0.9311	0.9228
C_{12} 10^{-11}	-0.8504	-0.4712	-0.8061	-0.8377	-0.8015	-0.8401

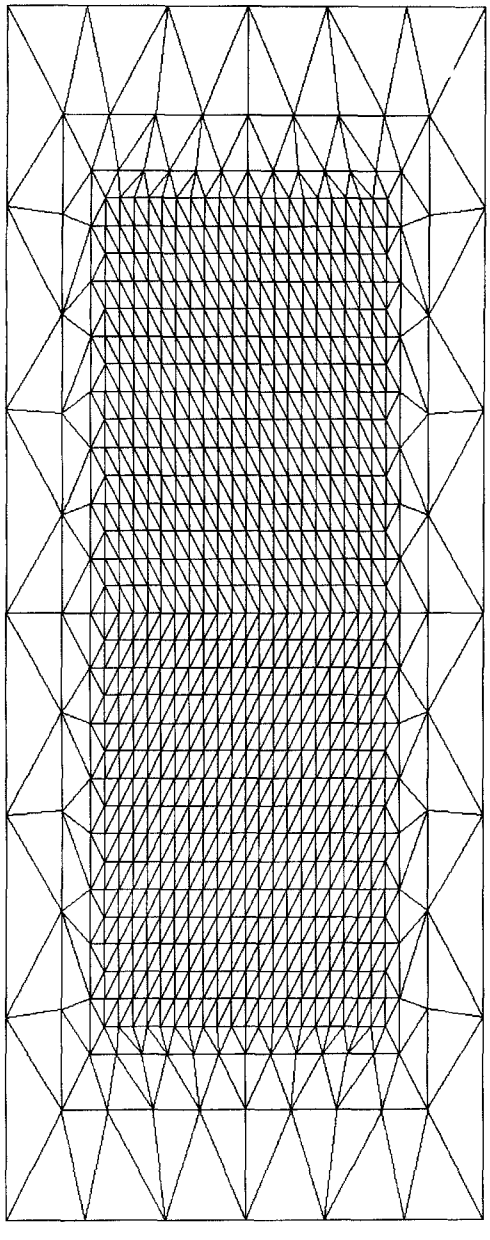

Fig. 3. Finite element mesh with transition layers.

$2M_0$ and the associated eigenvectors, which include the eigenvalues and the eigenvectors of transfer matrix X. Then we calculate

$$\det(R_1 - \lambda R_2) = \det\begin{pmatrix} K - \lambda A^T & -A \\ I & -\lambda I \end{pmatrix} = (-1)^n \det(-A + \lambda K - \lambda^2 A^T) \quad (17)$$

where det denotes the determinant of matrix. Because the matrix K is symmetric, (17) is a symmetric polynomial with respect to λ. If $\lambda \neq 0$ is a eigenvalue then $1/\lambda$ will be another one. It can be proved from (7) that all eigenvalues of X must be not greater than one, so it is easy to obtain the eigenvalues and the associated eigenvalues of X. Then X can be obtained from (15).

E. Proof of (7)

The scalar potential within the infinite region Ω_{out} satisfies the Laplace's equation. Assuming that the scalar potentials Φ_0 on Γ_0 is known, all scalar potentials within Ω_{out} can be uniquely determined. That is to say, Φ_1 can be uniquely determined by Φ_0. Because the Laplace's equation and the associated functional are linear, Φ_1 must be determined linearly by Φ_0. Then, there must exist a real matrix which satisfies

$$\Phi_1 = X\Phi_0. \quad (18)$$

Next, we take the linear transform $x' = \xi x$ and $y' = \xi y$, where ξ is the similar ratio between the layers of Ω_{out}. The positions of $\Gamma_0, \Gamma_1, \cdots, \Gamma_k$ now have been shifted to the position of $\Gamma_1, \Gamma_2, \cdots, \Gamma_{k+1}$, correspondingly. Since the scalar potentials on Ω_{out} have the identical values in different coordinate systems, the region within boundary Γ_0 and the one within Γ_1 have the same solutions if the initial condition on Γ_0 and Γ_1 are identical. Therefore, if the scalar potentials Φ_1 is known, Φ_2 can also be obtained

$$\Phi_2 = X\Phi_1. \quad (19)$$

Continuing to make the same linear transform, we can obtain the (7).

III. APPLICATION

Consider the two coupled microstrips shown in Fig. 2. Its finite element mesh is shown in Fig. 3. Because the number M_0 of boundary nodes is related to the stiffness matrix bandwidth and the computation time of the transfer matrix, some transition layers has been applied in Fig. 3. The capacitance matrix is calculated by the above method. Table I shows the numerical results obtained by the present method, together with those obtained by using a p.e.c shield, the ABC, the higher order ABC [4], infinite FEM [5], and other method [6]. Table I indicates that the present method can yield more accurate results.

IV. CONCLUSION

The above mentioned new FEM procedure is useful for two-dimension] and three-dimension electromagnetic Laplace's problems with open boundary. Because the whole region is discretized with infinite elements and no appropriate boundary is needed, the calculation error produced by the truncated boundary or absorbing boundary condition is avoided. The numerical results show that the calculation precision is very high.

REFERENCES

[1] A. Khebir, A. Kouki, and R. Mittra, "Asymptotic boundary conditions for finite element analysis of three dimensional line discontinuities," *IEEE Trans. Microwave Theory Tech.*, vol. 38, no. 10, pp. 1427–1432, 1990.

[2] F. R. Cooray and G. I. Costache, "An overview of the absorbing boundary conditions," *J. Electromagn. Waves Appl.*, vol. 5, no. 10, pp. 1041–1054, 1991.

[3] S. Pissanetzky, "A simple infinite element," *COMPEL-Int. J. Comput. Math. Elect. Eng.*, vol. 3, no. 2, pp. 107–114, 1984.

[4] A. Khebir and A. B. Kouki, "Higher order asymptotic boundary condition for the finite element modeling of two-dimensional transmission line structures," *IEEE Trans. Microwave Theory Tech.*, vol. 38, pp. 1433–1438, 1990.

[5] P. P. Silvester and R. L. Ferrari, *Finite Elements for Electrical Engineers*, 2nd ed. Cambridge: Cambridge Univ. Press, 1990.

[6] W. T. Weeks, "Calculation of coefficients of capacitance of multiconductor transmission lines in presence of a dielectric interface," *IEEE Trans. Microwave Theory Tech.*, vol. 18, pp. 35–43, 1970.

Thru Characteristics of a Coaxial Gap (FDTD Model and Measurements)

Bruce G. Colpitts

***Abstract*—Thru characteristics of a coaxial cable interrupted by a small gap are modeled and measured. Finite-difference time-domain (FDTD) modeling is applied in cylindrical coordinates to semirigid coaxial cable and to the intervening gap material. Both dispersive and nondispersive gap materials are investigated. Gap loss and phase shift are accurately predicted by this two-dimensional model which accounts for TEM and TM modes in the gap and coaxial apertures. An application of the model is to establish reference data for thin sample permittivity or moisture measurements.**

I. INTRODUCTION

A FDTD model in cylindrical coordinates is presented for a coaxial cable and intervening small gap. That is the cable is severed and a gap of up to one probe diameter (3.58 mm) is opened between the ends. Modeled results are verified with measurements to demonstrate accuracy for several gap sizes and materials. The coaxial gap is proposed as a sensor for very localized permittivity measurements of thin samples as an alternative to the coaxial reflection method which requires stacking of thin samples [1], [2] or the semiempirical approach used in [2] which requires two measurements of the same sample. Neither method is suitable for continuous thin sample moisture measurement. Since FDTD results are not readily invertible the procedure for determination of permittivity would be to characterize the gap response for a number of materials or moisture levels as part of calibration and to then use an interpolation procedure to determine the actual permittivity from the measured values. With sufficient computational speed an iterative solver would be feasible. This paper presents the FDTD numerical model along with measurements of two thin samples for verification. This presentation deals with the transmission response of the gap while in [3] the reflection properties of the coaxial cable have been considered and found to be accurately predicted by this approach. Now with the reflection and transmission properties well modeled and through the use of [4] one can either iteratively or through a look-up procedure determine the material properties.

Manuscript received September 6, 1994; revised October 2, 1995.

The author is with the Department of Electrical Engineering, University of New Brunswick, Fredericton, NB, Canada.

Publisher Item Identifier S 0018-9480(96)00462-0.

II. NUMERICAL ANALYSIS

A lossless and nondispersive cable dielectric is assumed while the gap material may have loss and dispersive characteristics. Dispersion is accounted for through recursive relations similar to those in [5]. The model is two-dimensional with the center of the center conductor forming a line of symmetry as in Fig. 1. This two-dimensional model accounts for TEM and TM modes at the apertures and throughout the gap but is not capable of modeling TE modes. This is not expected to be a limiting factor since the actual problem has circular symmetry and thus there are no mechanisms to excite TE modes [6]. Due to the small cable size chosen for this study and the need to precisely model gap details a cell size of 0.2 mm is chosen. This yields 52 cells from the inner conductor to the outer conductor in 3.58 mm (0.141") cable or 392 cells per wavelength at 26.5 GHz. With this small element size the Courant condition requires a correspondingly small time step, in the tens of picosecond range, depending upon the dielectric material selected. Field components used in this solution are the axial and radial electric fields and the circumferential magnetic field. Absorbing boundaries are of the first order Mur [7] type applied to the axial electric field while the line of symmetry is accounted for through symmetry of the magnetic field. Governing field equations in cylindrical coordinates are given in pseudo code form below for dispersive materials where the Debye equation and an additional conductivity term are used to describe their frequency dependent behavior as follows

$$\epsilon^*(\omega) = \epsilon_\infty + \frac{\epsilon_S - \epsilon_\infty}{1 + j\omega\tau_0} - j\frac{\sigma}{\omega\epsilon_0}. \tag{1}$$

Where the terms are defined as follows with their corresponding values for water at 25° shown in brackets, ϵ_∞ = permittivity at infinite frequency (4.9), ϵ_S= static permittivity (78.52), τ_0 = relaxation time (8.38×10^{-12}), σ = conductivity (0.0), and ω = angular frequency

$$HC^{n+1/2}(I,J) = HC^{n-1/2}(I,J) + F^*((EA^n(I+1,J) - EA^n(I,J)) - (ER^n(I,J+1) - ER^n(I,J)) \tag{2}$$

$$ER^{n+1}(I,J) = B^*ER^n(I,J) + C^*(HC^{n+1/2}(I,J-1) - HC^{n+1/2}(I,J)) + D^*SR^n(I,J) \tag{3}$$

$$SR^{n+1}(I,J) = A^*SR^n(I,J) + 0.5^*(A^*ER^n(I,J) + ER^{n+1}(I,J)) \tag{4}$$

$$EA^{n+1}(I,J) = B^*EA^n(I,J) + E^*(HC^{n+1/2}(I,J) - HC^{n+1/2}(I-1,J)) + C^*(HC(I,J) - HC(I-1,J)) + D^*SA^n(I,J) \tag{5}$$

$$SA^{n+1}(I,J) = A^*SA^n(I,J) + 0.5^*(A^*EA^n(I,J) + EA^{n+1}(I,J)) \tag{6}$$